Structural Engineering and Mechanics, *Vol. 63, No. 6 (2017) 847-856*
DOI: https://doi.org/10.12989/sem.2017.63.6.847

A comparative study on different walking load models

Jinping Wang[a] and Jun Chen[*]

Department of Structural Engineering, Tongji University, 1239 Siping Road, Shanghai, P.R. China

(Received October 12, 2016, Revised March 11, 2017, Accepted July 8, 2017)

Abstract. Excessive vibrations can occur in long-span structures such as floors or footbridges due to occupant's daily activity like walking and cause a so-called vibration serviceability issue. Since 1970s, researchers have proposed many human walking load models, and some of them have even been adopted by major design guidelines. Despite their wide applications in structural vibration serviceability problems, differences between these models in predicting structural responses are not clear. This paper collects 19 popular walking load models and compares their effects on structure's responses when subjected to the human walking loads. Model parameters are first compared among all these models including orders of components, dynamic load factors, phase angles and function forms. The responses of a single-degree-of-freedom system with various natural frequencies to the 19 load models are then calculated and compared in terms of peak values and root mean square values. Case studies on simulated structures and an existing long-span floor are further presented. Comparisons between predicted responses, guideline requirements and field measurements are conducted. All the results demonstrate that the differences among all the models are significant, indicating that in a practical design, choosing a proper walking load model is crucial for the structure's vibration serviceability assessment.

Keywords: walking load model; comparative study; long-span structures; vibration serviceability

1. Introduction

Due to wide application of high-strength light-weight construction materials and advanced construction technology, long-span floors are becoming increasingly popular in designs of public buildings like offices, shopping centers, convention centers and stadiums in order to provide multifunctional space. The long-span floors are characterized by their low vibration frequencies and low damping. As a result, they may experience strong vibrations caused by occupant's daily activities like walking or jumping when the human action's frequency is close to that of the floor (Rainer 1987). The vibration can be annoying to people on the floor, leading to the so-called vibration serviceability issue. To tackle this problem, many design guidelines require, in addition to the safety (strength) and static deflection assessment, vibration performance check for long-span floors at their design stage, such as AISC (Murray 1997), British Standard BS 5400 (1999), Japanese load code AIJ (2004) and Chinese code for design of concrete structures GB 50010-2010 (2015), to name a few. In some projects, the vibration serviceability issue can dominate the floor's structural design (Chen *et al*. 2015).

To fulfill the assessment task, in current design practice, the dynamic responses of a floor subjected to walking load are calculated and compared with design criteria. So far, extensive experimental studies have been conducted on walking load and many numerical models have been proposed. All these models differ from each other in many aspects including function forms, orders of components, dynamic load factors, phase angles and representative human body weights. It is easy to deduce that responses of a structure, when subjected to different walking models, are different. The degree of the differences, however, is not clear to design engineers, who usually select a load model objectively based on their own experience. Therefore, a comparative study on effects of all the walking load models in structural response calculation is imperative.

To this end, this study has collected 19 walking load models from literature and design guidelines, and conducted a thorough investigation on their influence on structural responses. Section 2 describes all the walking load models we gathered. General comparisons of all the models are presented in Section 3. Section 4 further compares these models using response spectra of a single-degree-of - freedom system (SDOF), followed by Section 5 as case studies. The main findings of this paper are summarized finally in Section 6.

2. Walking load models

We gathered 19 walking load models available in literature and various design guidelines. Almost all of these models are mathematically expressed by Fourier series function

$$F_p(t) = G + G\sum_{i=1}^{n} \alpha_{vi} \sin(2i\pi f_p t - \varphi_{vi}) \tag{1}$$

where G is the pedestrian's body weight (N), n is the order

∗Corresponding author, Professor
E-mail: cejchen@tongji.edu.cn
[a]Ph.D. Student
E-mail: 1510157@tongji.edu.cn

ISSN: 1225-4568 (Print), 1598-6217 (Online)

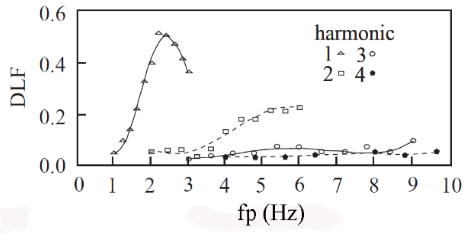

(a) DLF values for Rainer's model

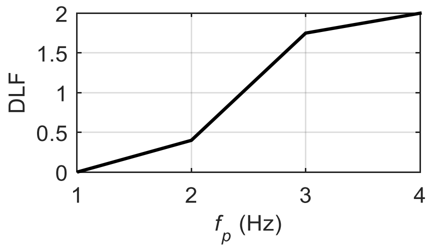

(b) DFL values of Yoneda's model

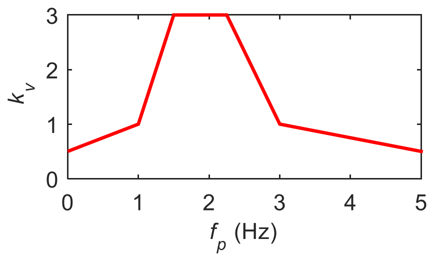

(c) k_v for Guidebook 2 for Eurocodes model

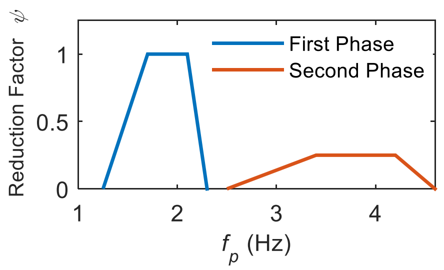

(d) Values of reduction factor for EN02 model

Fig. 1 Parameters of DLF values for four models

Table 1 Parameters of DLFs for first five (sub) harmonics for Živanović's model

Harmonic No. i	α_{vi} Mean	α_{vi} SD	Sub-harmonic No. i	α_{vi}^s
1	$-0.2649 f_p^3 + 1.3206 f_p^2 - 1.7597 f_p + 0.7613$	0.16	1	$0.026 \times \alpha_{v1} + 0.0031$
2	0.07	0.03	2	$0.074 \times \alpha_{v1} + 0.0100$
3	0.05	0.02	3	$0.012 \times \alpha_{v1} + 0.0160$
4	0.05	0.02	4	$0.013 \times \alpha_{v1} + 0.0093$
5	0.03	0.015	5	$0.015 \times \alpha_{v1} + 0.0072$

number of the function, α_{vi} is the Fourier's coefficient of the i th component which is usually called dynamic load factor (DLF), f_p is the walking frequency (Hz), φ_{vi} is the phase angle of the i th harmonic. Brief descriptions of these 19 models are given in this section. Unless otherwise specified, the values of DLF and phase angle of each model are listed in Table 2.

Blanchard *et al*. (1977) suggested a simple harmonic walking load model with merely the first harmonic. They also mentioned that for structures with natural frequency of 4-5 Hz, α_{vi} should be reduced and the second harmonic needs to be considered.

Bachmann and Ammann (1987) reported a five-order load model. Later, they proposed another walking load model, of which the DLF value for the first harmonic varies from 0.4 (at f_p=2.0 Hz) to 0.5 (at f_p=2.4 Hz) with linear interpolation in between. Rainer *et al*. (1987) suggested DLF values of the first four harmonics being determined according to Fig. 1(a) of the relationship between the DLF values and the walking frequency, which was obtained from experiment.

Allen and Murray (1993) presented a model in a slightly different form of Eq. (2), and DLF values can be obtained by Eq. (3). An updated version of the above model later appeared in 'Design Guide 11: Floor Vibration due to Human Activity' (Murray and Allen 1997) in the form of Eq. (4).

$$F_p(t) = P\left(1 + \sum_{i=1}^{n} \alpha_{vi} \cos 2i\pi f_p t\right) \tag{2}$$

where

$$\alpha_{vi} = 0.83 \exp(-0.35 i f_p) \tag{3}$$

$$F_i(t) = P\alpha_{vi} \cos(2i\pi f_p t) \tag{4}$$

Petersen (1996) put forward a model with three harmonics. DLF values and phase angles for three specific walking frequencies were given. Linear interpolation was recommended for values of other walking frequencies. Based on extensive experiments, Kerr (1998) suggested a three-order model in which DLF of the first harmonic was expressed by a polynomial function of walking frequency, DLFs of the second and third harmonics were taken as constant.

For footbridges, British standard BS 5400-2 (1999) suggested

$$F_p = 180 \sin(2\pi f_n t) \tag{5}$$

$$v_t = 0.9 f_n \quad \text{[m/s]} \tag{6}$$

As we can see, Eq. (5) represents an effective harmonic force due to walking which results in resonance response at the natural frequency f_n of a bridge. The maximum vertical acceleration of the bridge due to the pedestrian, who crosses the bridge at a specified speed v_t (Eq. (6)), should be lower than a threshold value. There is a reduction of threshold value by a factor varying linearly from 100% at f_n=4 Hz to 70% at f_n=5 Hz. The same approach was previously used by OHBDC (1983).

After collecting and analyzing a lot of experimental data, Arup (Willford *et al*. 2005) suggested a design value set in Table 2, taken from the statistical mean values of experiments plus 0.7 times of the standard deviations, representing a 25% probability of exceedance.

Yoneda (2002) advised a load model

Table 2 Single pedestrian vertical walking load models proposed by different authors

No.	Year	Scholar	DLFs	Phase angles	Body weight (N)	Walking frequency range
M1	1977	Blanchard	$\alpha_{v1}=0.257$	--	700	--
M2	1987	Bachmann & Ammann	$\alpha_{v1}=0.37$, $\alpha_{v2}=0.10$, $\alpha_{v3}=0.12$, $\alpha_{v4}=0.04$, $\alpha_{v5}=0.08$	--	--	2.0 Hz
M3	1988	Bachmann *et al.*	$\alpha_{v1}=0.4\sim0.5$ (linear interpolated with f_p) $\alpha_{v2}=\alpha_{v3}=0.1$	$\varphi_{v2}=\pi/2$ $\varphi_{v3}=\pi/2$	--	2.0-2.4 Hz
M4	1988	Rainer	α_{vi} given in Fig. 1(a)	--	735	1.7-2.3 Hz
M5	1993	Allen & Murray	$\alpha_{v1}=0.5$, $\alpha_{v2}=0.2$, $\alpha_{v3}=0.1$, $\alpha_{v4}=0.05$,	--	700	1.6-2.2 Hz
M6	1996	Petersen	$\alpha_{v1}=0.073$, $\alpha_{v2}=0.138$, $\alpha_{v3}=0.018$ $\alpha_{v1}=0.408$, $\alpha_{v2}=0.079$, $\alpha_{v3}=0.018$ $\alpha_{v1}=0.518$, $\alpha_{v2}=0.058$, $\alpha_{v3}=0.041$	$\varphi_{v2}=\varphi_{v3}=\pi/5$ $\varphi_{v2}=\varphi_{v3}=\pi/5$ $\varphi_{v2}=\varphi_{v3}=2\pi/5$	--	1.5 Hz 2 Hz 2.5 Hz
M7	1999	Kerr	$\alpha_{v1}=-0.265f_p^3+1.321f_p^2-1.760f_p+0.761$ $\alpha_{v2}=0.07$ $\alpha_{v3}=0.05$	--	--	1.6-2.2 Hz
M8	1999	BS 5400	$F_p=180\sin(2\pi f_p t)$	--	--	1.5-2.5 Hz
M9	2001	Arup	$\alpha_{v1}=0.41(f_p-0.95)\le0.56$, $\alpha_{v2}=0.069+0.0056(2f_p)$, $\alpha_{v3}=0.033+0.0064(3f_p)$, $\alpha_{v4}=0.013+0.0065(4f_p)$,	--	--	1-2.8 Hz 2-5.6 Hz 3-8.4 Hz 4-11.2 Hz
M10	2002	Yoneda	$F_p(t)=\alpha G\cos(2\pi f_p t)$ α given in Fig. 1(b)	--	700	--
M11	2004	Bro 2004	$F_p(t)=k_1k_2\sin(2\pi f_p t)$ $k_1=\sqrt{0.1BL}$, $k_2=150\ N$	--	--	--
M12	2004	Japanese Load Code	$\alpha_{v1}=0.4$, $\alpha_{v2}=0.2$, $\alpha_{v3}=0.06$	--	--	1.7-2.3 Hz
M13	2005	Guidebook 2 for Eurocodes	$F_p(t)=280k_v(f_n)\sin(2\pi f_n t)$ k_v given in Fig. 1(c)	--	700	1.0-3.0 Hz
M14	2006	French Guide	$\alpha_{v1}=0.4$, ($\alpha_{v1}=0.5$ for $f_p=2.4$ Hz) $\alpha_{v2}=\alpha_{v3}=0.1$	$\varphi_{v2}=\pi/2$ $\varphi_{v3}=\pi/2$	700	1.6-2.4 Hz
M15	2006	Živanović	see Table 1	--	750	--
M16	2007	Background document of EN02	$p(t)=P\cos(2\pi f_p t)\times n'\psi$ [N/m^2], $P=280\ N$ $F_p(t)=P\cos(2\pi f_p t)$ [N], ψ given in Fig. 1(d)	--	--	1.25-2.3 Hz
M17	2007	ISO 10137	$\alpha_{v1}=0.37(f_p-1.0)$, $\alpha_{v2}=0.1$, $\alpha_{v3}=0.06$, $\alpha_{v4}=0.06$, $\alpha_{v5}=0.06$	$\varphi_{vi}=\pi/2$ $f_n>if_p$ $\varphi_{vi}=0$ $f_n\le if_p$	750	1.2-2.4 Hz
M18	2009	Smith	$\alpha_{v1}=0.436(f_p-0.95)$ $\alpha_{v2}=0.006(2f_p+12.3)$ $\alpha_{v3}=0.007(3f_p+5.2)$ $\alpha_{v4}=0.007(4f_p+2.0)$	$\varphi_{v1}=0$ $\varphi_2=-\pi/2$ $\varphi_{v3}=\pi$ $\varphi_{v4}=\pi/2$	746	1.8-2.2 Hz 3.6-4.4 Hz 5.4-6.6 Hz 7.2-8.8 Hz
M19	2014	Chen	$\alpha_{v1}=0.2358f_p-0.2010$, $\alpha_{v2}=0.0949$, $\alpha_{v3}=0.0523$ $\alpha_{v4}=0.0461$, $\alpha_{v5}=0.0339$	$\varphi_1=-\pi/4$ $\varphi_{v4}=\pi/4$ $\varphi_{v5}=\pi/2$	--	1.2-3.0 Hz

$$F_p(t)=\alpha G\cos(2\pi f_p t) \tag{7}$$

where α (DLF) is obtained by curve in Fig. 1(b).

Swedish standard for design and construction of bridges, Bro 2004 (SRA 2004), assumed a stationary pulsating load model for the calculation of root-mean-square vertical acceleration of footbridges

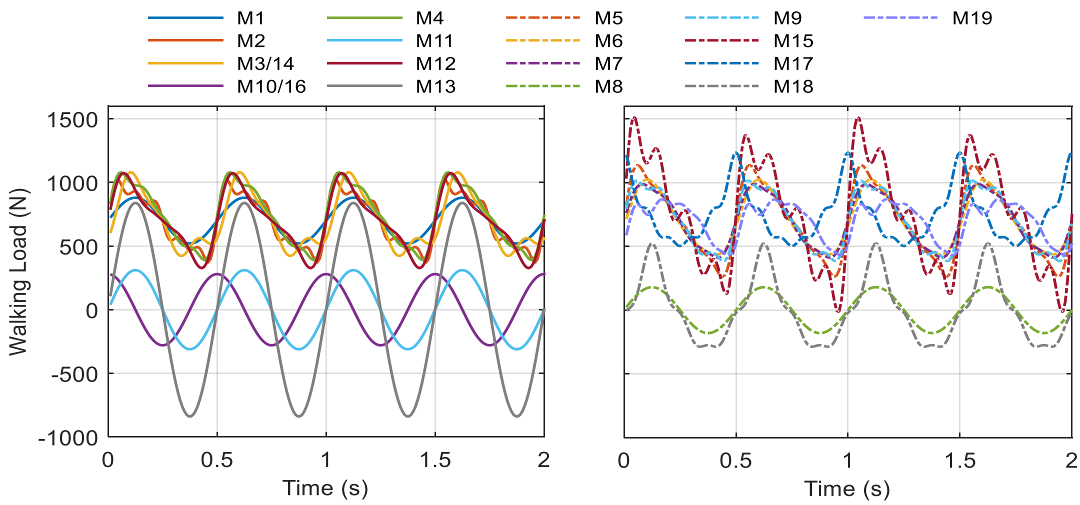

Fig. 2 Simulated walking load time histories of 19 different models at f_p=2.0 Hz

$$F_p(t) = k_1 k_2 \sin(2\pi f_p t) \tag{8}$$

where $k_1 = \sqrt{0.1BL}$, $k_2 = 150$ N are loading constants. B is the width of a bridge and L is the length of the bridge between supports.

Japanese load code (AIJ 2004) introduced a three-order model. Guidebook 2 for Eurocodes - Design of footbridges (Pietro 2005) recommended that pedestrian load could be defined by two separate models consisting of a concentrated force (as Eq. (9)) and a uniformly distributed load (as Eq. (10)) of vertical direction. $F_{n,v}(t)$ should be positioned at the most adverse point on the bridge deck, while $F_{s,v}(t)$ be applied on the whole deck of the bridge uniformly.

$$F_{n,v}(t) = 280k_v(f_v)\sin(2\pi f_v t) \text{ [N]} \tag{9}$$

$$F_{s,v}(t) = 15k_v(f_p)\sin(2\pi f_p t) \text{ [N/m}^2\text{]} \tag{10}$$

where k_v is the suitable coefficients of walking frequency according to Fig. 1(c).

The model adopted by French footbridge guide (Sétra 2006) has three harmonics and Živanović *et al*. (2007) put forward a stochastic model. The mean values and standard deviations describing the normal distributions of the first five harmonics are listed in Table 1. As for sub-harmonics, Živanović *et al*. established relationships between α_{vi}^{s} (DLF for the sub-harmonics) and α_{v1} (DLF for the first main harmonic), as presented in Table 1. Evidently, the magnitude of the DLF for the sub-harmonics can be obtained merely in the case that α_{v1} is known.

According to a background document for Eurocode 02 (Heinemeyer *et al*. 2007), the walking load model is expressed as

$$p(t) = P\cos(2\pi f_p t) \times n'\psi \text{ [N/m}^2\text{]} \tag{11}$$

$$F_p(t) = P\cos(2\pi f_p t) \text{ [N]} \tag{12}$$

This model is defined by a uniformly distributed harmonic load $p(t)$ [N/m^2] representing the equivalent pedestrian stream and a concentrated force $F_p(t)$ [N] standing for the harmonic load due to a single pedestrian. n' is the equivalent number of people walking simultaneously on the bridge. ψ is the reduction factor shown in Fig. 1(d). The value of P corresponding to vertical component is 280 N.

ISO 10137 (2007) also proposed a Fourier series in the form of Eq. (1). It recommended a conservative approach for the phase angle by introducing a phase lag of 90° for the harmonic contributions below resonance.

Similarly, 'Design of Floors for Vibration: A New Approach' (Smith 2007) introduced the walking excitation force having four harmonic components calculated from Fourier analysis given by

$$F_p(t) = \sum_h \alpha_h Q \sin(2\pi h f_p + \varphi_h) \tag{13}$$

where α_h can be obtained from Table 2, and static force exerted by an 'average person' with a weight of 746 N. Chen *et al*. (2014) proposed a five-order continuous walking load model featured with comprising sub-harmonics and all the model parameters were given based on experimental data.

Table 2 summarizes all computational details of the above 19 walking load models, hereafter denoted as M1-M19, including DLF values, phase angles, representative pedestrian weight and applicable walking frequency range.

3. General comparison

General comparison among models M1-M19 is discussed in this section in terms of model parameters, data source and applicable scope.

3.1 Model parameters

Fig. 2 compares the synthesized load time histories from the 19 models at the same walking frequency of 2 Hz. Calculation parameters follow each model's specific requirements, and for those that have not provided the body weight or phase angles, we use G=700 N and φ_{vi}=0. Note that the same rule for generating loads are also applied to calculations in Section 4 and Section 5.1.

It is seen from Fig. 2 that the 19 load curves differ from each other in the features like amplitude, number of peaks, mean value and variation pattern. This is not surprising given that these models have quite different model parameters as function orders, DLFs, representative body weight and phase angles. For instance, the order of function varies from one to five. Majority of the models consist of three or four harmonics. It is worth noting that the fourth and fifth harmonics are rarely significant where human perception is of concern, but may not be neglected for buildings accommodating vibration-sensitive instrument. The DLFs are either defined as constants or variables depending on walking frequency. Some models also consider contributions of sub-harmonics. The representative body weight values are given without their corresponding statistical significance, e.g. mean value of a population or a value with certain guarantee rate. Finally, phase angles are ignored in 13 of the total 19 models though they are very important in defining the variation pattern of the load. Furthermore, when it comes to crowd load, phase angles play a decisive part in dealing with crowd synchronization.

3.2 Data source

One aspect to explain the big differences among all the 19 models, as demonstrated in Fig. 2, is the data source. It is well acknowledged that a reliable load model relies heavily on a large number of real records, such as for earthquake and wind. Data source for developing many of the above walking models, however, are not distinct. Important experimental information is missing like number, age, gender and body weight of test subjects, test protocol (e.g., walking frequency range, interval and test sequence) and force measurement device adopted. For several models having clear data source, Table 3 compares their experimental conditions. Note that these experiments have significant difference in the experimental conditions. Moreover, some models are proposed based on the same data sources. A well-accepted test protocol seems to be necessary for further experimental investigations.

3.3 Applicable scope of the models

The applicable scope of the models are different, some are applicable only for footbridges, some for long-span floors and some for both. From the point of view of structural system, there are at least two main differences between footbridges and floors. First, the walking route and direction of a pedestrian (or a group) on a footbridge, because of its line-like shape, is predictable. Thus, the walking load path is known for numerical analysis of dynamic responses of the footbridge. For long-span floors, on the other hand, there are many possible routes and directions for a pedestrian. A most unfavorable situation must be selected before the analysis. Second, the long-span floors usually have closely-spaced modes of vibration due to their similar geometrical features in orthogonal directions. Therefore, contributions from multi-modes must be considered when assessing vibration performance of a floor, and consequently walking load models that can arouse higher modes of vibration are preferable. The vibration of a footbridge is usually dominated by one mode. Table 4 summarizes the applicable scope of all the walking models.

4. Comparison of response

The influence of the 19 models on structural responses is investigated in this section by comparing their response spectra. The main process is that, separately, apply each load model to a SDOF system with unit modal mass and a given damping ratio. The natural frequency of the system varies from 0.05 Hz to 12 Hz with an increment of 0.05 Hz, covering the extent of very soft to very stiff structures. In this study, the walking frequency is supposed as 2 Hz, damping ratio ζ=0.05. The calculation results are illustrated as Fig. 3 in which x label is natural frequency of the structure and y label is root mean square (RMS) of acceleration of steady state.

4.1 Peak responses

As illustrated in Fig. 3, when subjected with each model,

Table 3 Experimental conditions of several walking load models

No.	Scholar	Test subject			No. of records	Experimental Setup	Walking Freq. range
		Nationality	Number	Pedestrian Weight			
M14	Rainer *et al*.	Canadian	3	735 N (recommended)	--	17 m span floor strips	3.0 Hz
M10	Yoneda *et al*.	Japanese	--	700 N (recommended)	--	--	--
M7	Kerr	British	32 Male 8 Female	750 N (recommended)	882	Raised platform Force plates	1.0-3.0 Hz
M19	Chen *et al.*	Chinese	59 Male 14 Female	65.1 kg 54.2 kg	5004	3D motion capture 3D force plates	1.2-3.0 Hz
M15	James Brownjohn	--	1 Male 1 Male 1 Female	65 kg 62 kg 46 kg	30	Treadmill Force plates	2.5 km/h-7.5 km/h
	Živanović *et al*.	Based on Kerr's and Brownjohn's data					
M9	Arup	Mainly based on Kerr's data					

Table 4 Information of models from design codes and guidelines

No.	Scholar	Name of the references	Applicable scope
M1	Blanchard *et al.*	Design criteria and analysis for dynamic loading of footbridges	Bridges with $f_n < 4$ Hz
M4	Rainer *et al.*	Dynamic loading and response of footbridges	Footbridges with $f_n < 10$ Hz
M5	Allen & Murray	Floor vibrations vue to human activity	Floor and bridges
M6	Petersen	Dynamik der Baukonstruktionen	Footbridges
M7	Kerr	Human induced loading on staircases	Footbridges
M8	BS 5400	Steel, concrete and composite bridges	Foot or cycle track bridges
M9	Arup	Improved floor vibration prediction methodologies	Floors and bridges
M10	Yoneda *et al.*	Simplified method to evaluate pedestrian-induced maximum response of cable-supported pedestrian bridges	Footbridges
M11	Bro 2004	Vägverkets allmänna tekniska beskrivning för nybyggande och förbättring av broar -	Bridges with $f_n \geq 3.5$ Hz
M12	Japanese Load Code	Recommendations for loads on buildings	Buildings
M13	Guidebook 2 for Eurocodes	Design of bridges	Footbridges
M14	French Footbridges Guide	Technical guide-foodbridges – Assessment of vibrational behavior of footbridges under pedestrian loading	Footbridges
M15	Živanović *et al.*	Probability-based prediction of multi-mode vibration response to walking excitation	Slender footbridges
M16	Background document of EN02	Design of lightweight footbridges for human induced vibrations	Footbridges
M17	ISO 10137	Human exposure to continuous and shock-induced vibrations in buildings	Buildings and walkways
M18	Smith *et al.*	Design of floors for vibration: a new approach	All steel-framed floor and building types

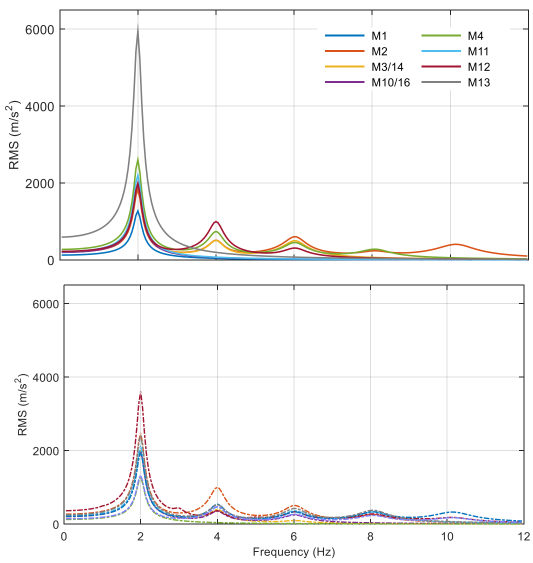

Fig. 3 Responses spectra of all 19 walking load models (walking frequency of 2 Hz, modal mass of 1 kg and damping ratio 0.05)

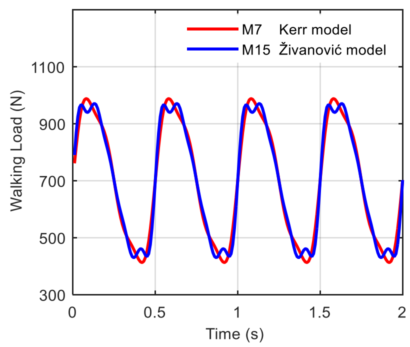

(a) Simulated walking load time history

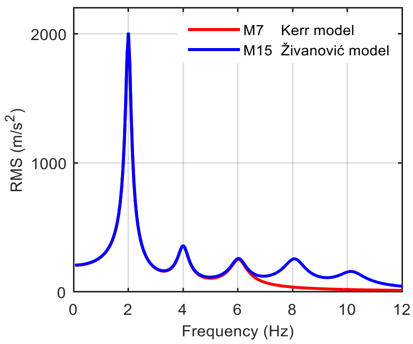

(b) RMS

Fig. 4 Kerr's and Živanović's (mean values as DLFs) models at f_p=2 Hz, mass of 1 kg and ζ=0.05

the structure presents a fair large disparity in peak acceleration response. At the natural frequency of 2 Hz, the ratio of the maximum response among all the load models (Guidebook 2 for Eurocodes model) and the minimum

Table 5 Ratios of DLF and RMS at the points of frequency multiplication

Order	1				2			
Model	M2	M17	M19	Ratio	M2	M17	M19	Ratio
DLF	0.37	0.37	0.271	1:1.00:0.73	0.1	0.1	0.0949	1:1.00:0.95
RMS (m/s^2)	1835	1834	1334	1:1.00:0.73	514	506	477	1:0.98:0.93
Order	3				4			
Model	M2	M17	M19	Ratio	M2	M17	M19	Ratio
DLF	0.12	0.06	0.0523	1:0.50:0.44	0.04	0.06	0.0461	1:1.50:1.15
RMS (m/s^2)	603	312	269	1:0.51:0.45	237	310	235	1:1.32:0.99

response (Blanchard's model) is 4.669. When the natural frequency is 4 Hz, ratio of the maximum response (Allen and Murray's model) and the minimum (Blanchard's model) reaches more than 20. Thus, though the responses of each load model share roughly the same tendency, the corresponding peak RMS accelerations vary a lot in values.

4.2 The influence of orders of the models

Merely considering the mean values of main harmonics of Živanović's model as its DLFs, Kerr's and Živanović's models share the same first two dynamic load factors, but Živanović's model has three additional harmonic components. To exclude the effect of phase angles, here all the phase angles are assigned zero. The load time history and RMS response spectrum are shown in Fig. 4.

From Fig. 4(a), DLFs of higher orders have an effect on load time history; as for Živanović's model, twin peaks occur; for Kerr's model there is only one peak value in every load cycle. In the response spectrum (Fig. 4(b)), when the system is at one and two times of walking frequency, the peaks appear and roughly share the same value; when the system is at three, four and five times of walking frequency, there exist peaks in Živanović's model while no peak in Kerr's. Hence, for structural frequency corresponding to the same contributing harmonic components of different models, there is rarely distinction; for that of higher orders, there are obvious distinctions.

4.3 The influence of dynamic load factors

Making a comparison of Bachmann and Ammann's (1987), ISO 10137 (2007) and Chen's (2014) models who possess the same orders of harmonics, but different DLF values, the results can be seen in Figs. 2-3 curve M2, curve M17 and curve M19, based on which Table 5 is produced. All phase angles are set zero in the calculation.

Noting that in accordance with Table 2, the ratios of DLFs are approximately equal to the corresponding ratios of RMS. In other words, when natural frequency of a structure is of a certain integer multiple of walking frequency, RMS of the structure is in proportion to the same integer multiple order of DLF with respect to different models.

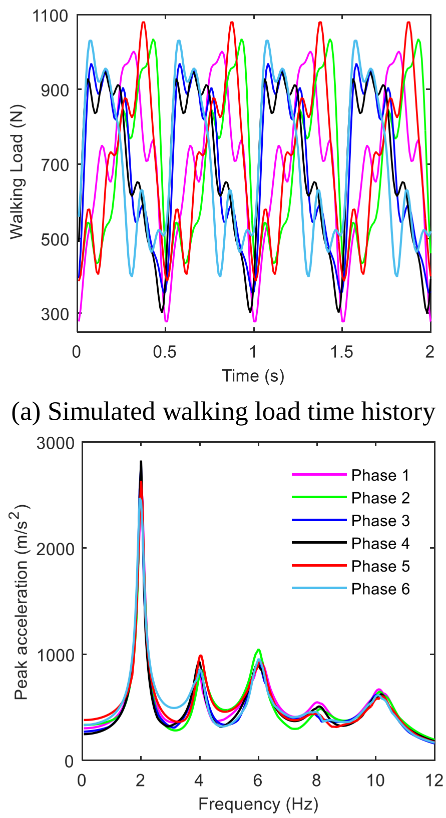

(a) Simulated walking load time history

(b) RMS

Fig. 5 Six random phase cases of Bachmann and Ammann's model at f_p=2 Hz, mass of 1 kg and ζ=0.05

4.4 The influence of phase angles

Take different phase angles of Bachmann and Ammann's model (Bachmann and Ammann 1987) to carry on this analysis. Phase angle values of this model are taken randomly within [0, π]. The result is presented in Fig. 5. In terms of structural responses, the difference is not obvious, especially in peak acceleration (Fig. 5(b)).

4.5 The influence of the function form

Almost all the walking load models have been proposed based on Fourier decomposition. However, some of these models are composed of the pedestrian's body weight as a constant term and a combination of harmonic forces while some do not include the constant term such as BS 5400 code, Yoneda's, Pietro's and background document of EN02 models. Take Blanchard's and BS 5400 models as an example. The amplitudes of the two Fourier decomposition expressions are the same. Results are shown as Figs. 2-3 curve M1 and curve M8.

Though the two load time histories as curve M1 and curve M8 in Fig. 2 seem entirely different, they have barely any disparity in shape. That is because M8 does not contain the body weight, while M1 does. In addition, the structural responses have substantially the same tendency. It is not hard to explain this: a constant term of a load only has great influence on displacement of a structure, but no influence

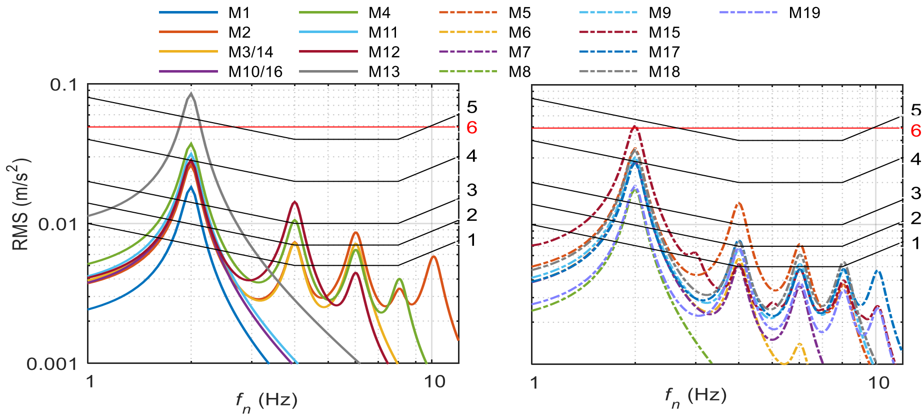

(a) RMS at f_p=2 Hz, modal mass of 70 t, damping 0.05

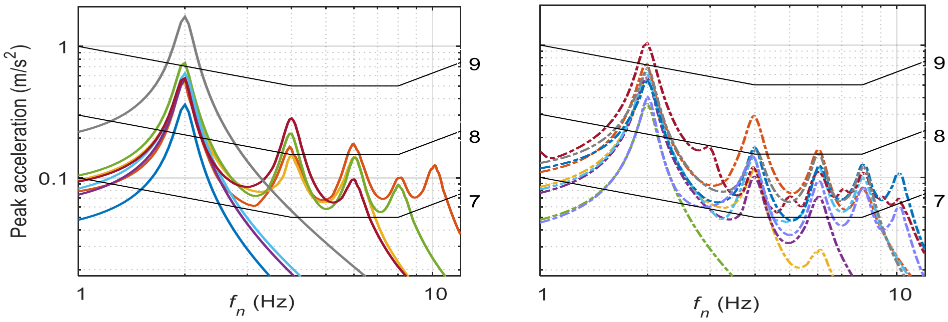

Curve 1: Critical baseline
Curve 2: Residential for night
Curve 3: Residential for day lower limit
Curve 4: Office and residential for day upper limit
Curve 5: Workshop
Curve 6: Ellingwood and Talling's criterion for shopping malls
Curve 7: Office, residential
Curve 8: Indoor footbridge, Shopping mall, Dining and Dancing
Curve 9: Rhythmic activities and outdoor footbriges

(b) Peak acceleration at f_p=2 Hz, mass 5 t, damping 0.05

Fig. 6 Structural response in logarithm scale of different models at f_p=2 Hz and vibration criteria

on accelerations. Besides, it also proves that DLF contributes largely to the structural response.

5. Case study

5.1 Comparison with design criterion

Many criteria for human comfort have been proposed over the years. To make a comparison on the different models when encounter different criteria, we consider two examples here: one structure has a modal mass of 70 t and the other structure has a modal mass of 5 t, supposing that a structure's vibration due to walking load is dominated by one mode. For both cases, the natural frequency of the dominating mode is 2.0 Hz and the damping ratio is 0.05. The response spectra obtained from the two structures applied on the 19 load models are shown in Figs. 6(a)-(b), respectively.

The commonly adopted design criterion curves for nine different scenarios are also depicted in Fig. 6 for comparison purpose (Murray 1997, Ellingwood 1984, BS 6472 1992, ISO 10137 2007).

Noting from Fig. 6(a) that for one given criteria (say curve 4 of daytime upper response limit for office and residential buildings), assessment of several load models (M13, M15, M18 etc.) indicates that most occupants on the building would perceive annoying vibration (i.e., negative assessment result), while others (M19, M8, M17 etc.) believe that majority of the occupants would be unaware of the vibration (i.e., positive assessment result). The same conclusion can be made for Fig. 6(b) that different models may lead to completely opposite assessment result.

5.2 Comparison with field measurements

To do some experimental verification, a 10 m×6 m rectangular concrete floor was constructed which casted in place with concrete grade C40 of 110 mm in thickness. It was simply supported at two ends of the long span and dynamic characteristics of the floor were extracted from the measurements. The natural frequencies of the first four vibration modes are 3.52, 6.16, 8.97, 13.19 Hz, and the corresponding modal masses are 8583, 2587, 9625 and 2423 kg (Liu and Chen 2014). Test data was obtained from record of seven accelerometers (Lance LC0132T, USA) installed beneath the floor.

Single person walking test was conducted on the floor: a

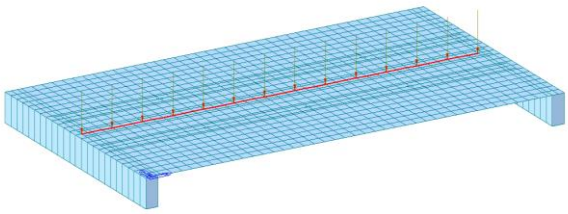

Fig. 7 Finite element model of the floor and load exerting method

test subject weighed 813.4 N was required to walk straight on the midline along the long span at walking frequencies guided by a metronome, with stride of about 0.75 m, same as the path in Fig. 7. One of the test response time histories at walking frequency of 1.75 Hz is shown in Fig. 8 which is obtained from record of the accelerometer at the floor center. Details of field measurements of this floor can be found in Liu and Chen's paper (2014). We then applied the 19 walking load models (with the same walking frequency 1.75 Hz) on a finite element model of this floor (Fig. 7) established by a software, Midas-Gen, to calculate its dynamic responses.

Walking load as expressed by Eq. (1) can be translated as a point force exerted on the floor, as a function of time and pedestrian position. Noting that x is the pedestrian position in relation to the structure, the load of a pedestrian moving at constant speed v can therefore be represented as the product of a time component $F(t)$ by a space component $\delta(x - vt)$, where δ being the Dirac operator, defined as

$$P(x,t) = F(t)\delta(x - vt) \tag{14}$$

Based on this, the load exerting method on the finite element model is illustrated in Fig. 7.

The acceleration at the center point of the floor was extracted for each model. Peak acceleration, maximums of 1 s RMS and 10 s RMS and RMS along the whole time calculated from the finite element model were normalized with the corresponding values from field measurements (the last row in Table 6, denoted with an asterisk), as listed in Table 6.

Taking peak acceleration values as comparison variable, six models (M2, M6, M7, M9, M15, and M19, those marked in grey) lead to a prediction having less than 15% error to the measured response. The other models, however, can lead to either significant overestimation or serious underestimation for this particular case. One common feature for those models seriously underestimating the response (M8, M10, M11, M13 and M16) is that they only focus on the first harmonic of the Fourier series, but actually, this testing floor with the fundamental frequency of 3.52 Hz was resonant to the walking loads (f_p=1.75 Hz) at twice the walking frequency. Thus, these models only suit for structures with fundamental frequency within the common range of human walking frequency. This jumps to the same conclusion with Section 4.2.

In addition, it is not hard to find that M5 and M12 show greater response than other models. Back to the functions of the models, we can see that this phenomenon accounts for

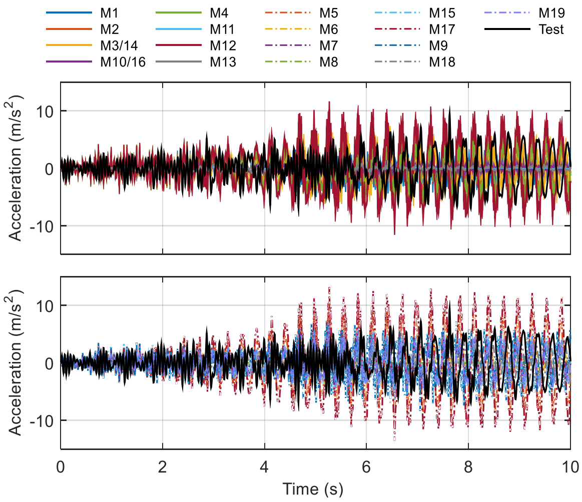

Fig. 8 Walking response time histories of 19 models and test case at f_p=1.75 Hz

Table 6 Response of acceleration ratio between 19 walking load models and the test result

Model	RMS	Max. of 1 s RMS	Max. of 10 s RMS	Peak Acc.
Test	1	1	1	1
M1	0.7294	0.8068	0.7654	0.8277
M2	1.3320	1.0282	1.1072	1.1482
M3	1.1485	0.8293	0.9158	0.8124
M4	1.2967	1.0272	1.0936	1.1554
M5	2.2954	1.4357	1.7703	1.4307
M6	1.3292	0.9726	1.0699	1.0739
M7	1.0718	0.9214	0.9459	1.0344
M8	0.0313	0.0301	0.0281	0.0276
M9	1.2264	0.9761	1.0368	1.0974
M10	0.2566	0.2828	0.2682	0.2949
M11	0.0541	0.0519	0.0486	0.0477
M12	2.2917	1.4316	1.7655	1.4228
M13	0.1461	0.1403	0.1312	0.1287
M14	1.1492	0.8312	0.9170	0.8144
M15	1.1233	1.0086	1.0182	1.1187
M16	0.2933	0.3232	0.3065	0.3370
M17	1.5058	1.1978	1.2727	1.3630
M18	1.0864	0.6534	0.8230	0.3910
M19	1.1755	0.8403	0.9379	0.9271
Test (cm/s^2)*	1.7337	3.9832	2.9349	9.5088

*Values in the last row are the absolute experimental measurement values in cm/s^2.

the DLF values of these two models being larger than the rest. We can say: for structures with natural frequencies among the common range of f_p, DLF is the most significant factor of walking load.

6. Conclusions

Vibration serviceability problem due to human-induced loads becomes an important, even dominate design issue for long-span and flexible structures like floors and footbridges. Many load models are available for engineers when designing such structures. However, the differences among these models in predicating a structure's dynamic responses are not clear. To solve this problem, this paper has collected 19 walking load models. These models are compared against each other in terms of model parameters and structural response. Among all the model factors discussed, the DLF values are the most important one for peak structural responses, the phase angle has little effect on structural response due to an individual walking but is very important for describing synchronization of a walking crowd.

The comparisons reveal that different load models will lead to significantly different structural responses that can either be overestimation or underestimation compared with the field measured response, and can therefore result in opposite assessment conclusions. This difference can be explained by different function form, model parameters, data source and applicable scope among all the models. Therefore, it is difficult to select one best model from all the 19 models. Nevertheless, the present comparison studies indicate that it is better to try more load models, besides that specified in certain design guidelines for structural vibration serviceability assessment, and those models considering contributions of higher harmonics might be proper for designing structures with multi-mode vibration. It is of great significance to concern with the applicable scope of every model in ahead. What is more, a well-accepted test protocol is necessary for further experimental investigations and is important for developing the next generation of walking load model.

Acknowledgements

Financial supports from the National Natural Science Foundation (51478346) and State Key Laboratory for Disaster Reduction of Civil Engineering (SLDRCE14-B-16) to this research are highly appreciated.

References

AIJ (2004), *Recommendations for Loads on Buildings*, Japan.

Allen, D.E. and Murray, T.M. (1993), "Design criterion for vibrations due to walking", AISC *Eng. J.*, **30**(4), 117-129.

Bachmann, H. and Ammann, W. (1987), "Vibrations in structures induced by man and machines", *Can. J. Civil Eng.*, **15**(6), 1086-1087.

Blanchard, J., Davies, B.L. and Smith, J.W. (1977), "Design criteria and analysis for dynamic loading of footbridges", *Proceeding of a Symposium on Dynamic Behaviour of Bridges at the Transport and Road Research Laboratory*, Berkshire, May.

Bro 2004 (2004), *Vägverkets Allmänna Tekniska Beskrivning för Nybyggande och Förbättring av Broar, Svensk Byggtjänst,* Stockholm, Sverige.

Brownjohn, J.M.W., Pavić, A. and Omenzetter, P. (2004), "A spectral density approach for modelling continuous vertical forces on pedestrian structures due to walking", *Can. J. Civil Eng.*, **31**(1), 65-77.

BS 5400 (1999), *Steel, Concrete and Composite Bridges - Part 2: Specification for Loads*, BSI, London, UK.

BS 6472 (1992), *Evaluation of Human Exposure to Vibration in Buildings (1 Hz to 80 Hz)*, BSI, London, UK.

Chen, J., Wang, H.Q. and Peng, Y.X. (2014), "Experimental investigation on Fourier-series model of walking load and its coefficients", *J. Vib. Shock,* **33**(8), 11-15.

Chen, J., Zhang, M. and Liu, W. (2015), "Vibration serviceability performance of an externally prestressed concrete floor during daily use and under controlled human activities", *J. Perform. Constr. Facil.*, **30**(2), 04015007.

Ellingwood, B. and Tallin, A. (1984), "Structural serviceability: floor vibrations", *J. Struct. Eng.*, **110**(2), 401-419.

GB 50010-2010 (2015), *Code for Design of Concrete Structures*, China Architecture & Building Press, Beijing, China.

Heinemeyer, C. *et al*. (2007), *Design of Lightweight Footbridges for Human Induced Vibrations*, European Commission, Italy.

ISO 10137 (2007), *Bases for Design of Structure-Serviceability of Buildings and Walkways against Vibrations*, Geneva.

Kerr, S.C. (1998), "Human induced loading on staircases", PhD Dissertation, University of London, University College, London.

Liu, W. and Chen, J. (2014), "Vibration serviceability analysis of external-prestressing concrete floor through field measurements and experiments", *Proceedings of the 13th International Symposium on Structural Engineering*, Hefei, October.

Murray, T.M., Allen, D.E. and Ungar, E.E. (1997), "Floor vibrations due to human activity", *Nature News,* **17**(7), 768-771.

OHBDC (1983), *Ontario Highway Bridge Design Code*, Alexandria.

Petersen, C. (1996), "Dynamik der Baukonstruktionen", Vierweg, Braunschweig /Wiesbaden.

Pietro, C. *et al.* (2005), *Guidebook 2- Design of Bridges of Eurocode*, Czech Technical University, 166 08 Prague 6, Prague, Czech Republic.

Rainer, J.H., Pernica, G. and Allen, D.E. (1987), "Dynamic loading and response of footbridges", *Can. J. Civil Eng.*, **15**(1), 66-71.

Smith, A.L., Hicks, S.J. and Devine, P.J. (2007), *Design of Floors for Vibration: A New Approach*, The Steel Construction Institute, Silwood Park, Ascot, Berkshire, UK.

The Sétra (2006), *Assessment of Vibrational Behavior of Footbridges under Pedestrian Loading-Practical Guidelines*, the Sétra, Paris, France.

Willford, M., Young, P. and Field, C. (2005), "Improved methodologies for the prediction of footfall-induced vibration", *Proceedings of SPIE 5933, Buildings for Nanoscale Research and Beyond,* California.

Yoneda, M.A. (2002), "Simplified method to evaluate pedestrian-induced maximum response of cable-supported pedestrian bridges", *Proceedings of the International Conference on the Design and Dynamic Behavior of Footbridges,* Paris.

Živanović, S., Pavić, A. and Reynolds, P. (2007), "Probability-based prediction of multi-mode vibration response to walking excitation", *Eng. Struct.*, **29**(6), 942-954.